



Estimating total heliospheric magnetic flux from single-point in situ measurements

M. J. Owens,^{1,2} C. N. Arge,³ N. U. Crooker,¹ N. A. Schwadron,¹ and T. S. Horbury⁴

Received 12 August 2008; revised 18 September 2008; accepted 6 October 2008; published 11 December 2008.

[1] A fraction of the total photospheric magnetic flux opens to the heliosphere to form the interplanetary magnetic field carried by the solar wind. While this open flux is critical to our understanding of the generation and evolution of the solar magnetic field, direct measurements are generally limited to single-point measurements taken in situ by heliospheric spacecraft. An observed latitude invariance in the radial component of the magnetic field suggests that extrapolation from such single-point measurements to total heliospheric magnetic flux is possible. In this study we test this assumption using estimates of total heliospheric flux from well-separated heliospheric spacecraft and conclude that single-point measurements are indeed adequate proxies for the total heliospheric magnetic flux, though care must be taken when comparing flux estimates from data collected at different heliocentric distances.

Citation: Owens, M. J., C. N. Arge, N. U. Crooker, N. A. Schwadron, and T. S. Horbury (2008), Estimating total heliospheric magnetic flux from single-point in situ measurements, *J. Geophys. Res.*, *113*, A12103, doi:10.1029/2008JA013677.

1. Introduction

[2] Line-of-sight photospheric magnetic flux is routinely measured by ground- and space-based magnetograms. A significant fraction of this flux is “closed,” meaning that it forms loops below the height at which gas pressure exceeds magnetic pressure and thus does not contribute to the interplanetary magnetic field carried by the solar wind [e.g., Wang and Sheeley, 2003]. The foot points of “open” magnetic field lines, which extend high enough to be dragged out by the solar wind and contribute to the heliospheric magnetic flux, are strongly associated with coronal holes [e.g., Levine et al., 1977; Wang et al., 1996]. Direct measurement of this open magnetic field component is generally limited to single-point heliospheric measurements taken by in situ spacecraft, from which total heliospheric flux is then deduced.

[3] On the basis of such heliospheric flux estimates, a number of models for the evolution of the heliospheric magnetic field have been put forward. Fisk et al. [1999] suggest that the Sun’s open flux tends to be conserved, with “interchange reconnection” [Crooker et al., 2002] between open and closed fields resulting in an effective diffusion of open flux across the solar surface, without any net change in the total open flux. This allows the heliospheric field to

evolve as a simple rotation of regions of positive and negative polarity separated by a single, large-scale heliospheric current sheet [Fisk and Schwadron, 2001], which is one explanation for the available observations [Jones et al., 2003]. Alternatively, it has been argued that emerging midlatitude bipoles cause closed coronal loops to rise and destroy or create open flux in such a way as to reverse the coronal field [Babcock, 1961; Wang and Sheeley, 2003]. Transient events may also have a significant role in the evolution of the heliospheric magnetic field [Low, 2001]. Indeed, Owens et al. [2007] suggest that the migration of open flux is facilitated by reconnection with the magnetic field systems of coronal mass ejections (CMEs). The flux injected into the heliosphere by CMEs may also explain the solar cycle variation in total heliospheric flux inferred from near-Earth single-point spacecraft measurements [Owens and Crooker, 2006, 2007].

[4] Clearly, the assumption that single-point spacecraft measurements are sufficient to estimate total heliospheric magnetic flux has wide-reaching implications for our understanding of heliospheric evolution. The unique polar orbit of the Ulysses spacecraft, with an aphelion (perihelion) of 5.4 (1.3) AU, allows the only high-latitude observations of the heliospheric magnetic field [Balogh et al., 1992]. The validity of the single-point approximation rests largely on Ulysses observations of a latitude invariance in $R^2|B_R|$ [Smith and Balogh, 2003; Lockwood et al., 2004], where R is the heliocentric distance and B_R is the radial component of the magnetic field. Thus, at any point in the heliosphere $4\pi R^2|B_R|$ should be representative of the total heliospheric flux. Only data from 2-year periods covering Ulysses perihelion passes were considered in the latitude invariance reported by Smith and Balogh [2003] and Lockwood et al. [2004], as flux estimates at large heliocentric distance are complicated by a reduced “signal to noise” (E. Smith,

¹Center for Space Physics, Boston University, Boston, Massachusetts, USA.

²Now at Space and Atmospheric Physics, Blackett Laboratory, Imperial College London, London, UK.

³Space Vehicles Directorate, Air Force Research Laboratory, Kirtland Air Force Base, New Mexico, USA.

⁴Space and Atmospheric Physics, Blackett Laboratory, Imperial College London, London, UK.

Table 1. Spacecraft Separated From Earth by More Than 10° in Heliolatitude or Heliolongitude Used in This Study^a

Spacecraft	Magnetometer	Data Used for Total Flux Estimates			
		Years ^b	R ^c	Longitude Separation ^d	Latitude Separation ^d
Pioneer 6	<i>Ness et al.</i> [1966]	1965–1966	0.8–1 AU	77°	4°
Pioneer 7	<i>Ness et al.</i> [1966]	1966–1967	1–1.1 AU	113°	5°
Pioneer 10	<i>Smith et al.</i> [1975]	-	-	-	-
Pioneer 11	<i>Smith et al.</i> [1975]	1973	1.1–2.2 AU	118°	5°
Helios 1	<i>Scarce et al.</i> [1975]	1974–1981	0.3–1 AU	180°	14°
Helios 2	<i>Scarce et al.</i> [1975]	1976–1980	0.3–1 AU	180°	14°
Voyager 1	<i>Behannon et al.</i> [1977]	1977	1.3–1.8 AU	18°	3°
Voyager 2	<i>Behannon et al.</i> [1977]	1977–1978	1.3–2.2 AU	54°	6°
Pioneer Venus Orbiter	<i>Russell et al.</i> [1980]	1978–1988	0.72 AU	180°	11°
ICE (ISEE 3)	<i>Frandsen et al.</i> [1978]	1984–1990	0.93–1 AU	71°	8°
Ulysses	<i>Balogh et al.</i> [1992]	1990–2008	1.3–2.2 AU	180°	87°
NEAR	<i>Acuña et al.</i> [1997]	1997–2000	1–1.8 AU	175°	16°
STEREO A	<i>Acuña et al.</i> [1997]	2007–2008	0.96 AU	27°	3°
STEREO B	<i>Acuña et al.</i> [2007]	2007–2008	1.1 AU	24°	3°

^aBecause of the strong radial variation in estimated heliospheric flux (see Figure 1), flux estimates are further limited to measurements at $R < 2.5$ AU, as shown by the right-hand side of the table.

^bThe time period over which data are used.

^cThe heliocentric distance covered by the spacecraft during this period.

^dThe maximum heliographic longitude and latitude separation from Earth and, hence, the OMNI spacecraft.

personal communication, 2008): as R increases, the magnetic field becomes increasingly azimuthal, increasing the uncertainty in the estimated flux. *Smith and Balogh* [2003] also reported little difference in $R^2|B_R|$ between the solar minimum (1994–1996) and maximum (2000–2002) perihelion passes, contrary to the in-ecliptic observed solar cycle variation in flux [e.g., *Richardson et al.*, 2002], but ascribed this apparent time invariance to the solar maximum observation occurring during a temporary, global decrease. This temporary solar maximum drop in heliospheric flux was also seen in near-Earth data (the so-called “Gnevyshev gap” [*Gnevyshev*, 1977]). In general, we note that identification of true solar cycle variations in the Ulysses data are complicated by the Ulysses orbit, which results in a radial distance variation almost in phase with the solar cycle.

[5] Estimates of total heliospheric flux are possible using models constrained by the observed photospheric magnetic field. Potential field [e.g., *Schatten et al.*, 1969; *Altschuler and Newkirk*, 1969] and magnetohydrodynamic solutions [e.g., *Linker et al.*, 1999; *Mikić et al.*, 1999] of total heliospheric flux generally show reasonable agreement with single-spacecraft measurements [*Wang and Sheeley*, 2003; *Owens et al.*, 2008; *Lepri et al.*, 2008]. However, uncertainties in the systematic offsets in the magnetograms [*Svalgaard et al.*, 1978; *Ulrich*, 1992; *Wang and Sheeley*, 1995], as well as the underlying model assumptions and tuning, mean that such modeling may not provide an adequate or independent test of the single-point assumption [*Lockwood et al.*, 2004]. Estimates of heliospheric magnetic flux based upon geomagnetic indices [e.g., *Lockwood et al.*, 1999; *Svalgaard and Cliver*, 2007] are generally derived from single-point magnetic field measurements and thus do not provide an independent test.

[6] In this study, we directly test the assumption that single-point measurements are sufficient to estimate total heliospheric flux by comparing the estimates by well-separated spacecraft in the heliosphere. The inclination of the ecliptic plane to the heliographic equator allows sam-

pling of latitudinal separations up to $\sim 14.5^\circ$ with a variety of spacecraft over long time periods. Longitudinal and radial variations in B_R are assumed to be averaged out by considering time periods longer than a solar rotation. This assumption is valid if total heliospheric flux is not varying on timescales less than a solar rotation, which is tested by using spacecraft at large longitudinal and radial separations.

2. Methodology

2.1. Flux Calculation

[7] We consider the total heliospheric flux content to be the unsigned flux content threading a heliocentric sphere [e.g., *Smith and Balogh*, 2003]. Note that some studies [e.g., *Lockwood et al.*, 1999] instead compute the amount of flux of a single polarity, a factor 2 lower than the total unsigned flux. If $R^2|B_R|$ is invariant throughout the heliosphere, the calculation of total heliospheric flux, Φ_{TOTAL} , from single-spacecraft observations is straight forward:

$$\Phi_{\text{TOTAL}} = 4\pi R^2 \langle |B_R| \rangle. \quad (1)$$

Care must be taken, however, in the calculation of the time average of the radial field ($\langle B_R \rangle$), as the bipolar nature of B_R means that $|\langle B_R \rangle| \neq \langle |B_R| \rangle$. *Smith and Balogh* [2003] showed that this effect is probably insignificant if longer-term averages are based on $|B_R|$ over shorter intervals (an hour was deemed sufficient). For the Ulysses data set, we too find little difference in Carrington rotation flux estimates based on 5-min and 1-h data). Thus, to compare total flux computed from different data sets, which frequently have different intrinsic time resolutions, we first compute $\langle B_R \rangle_{1h}$ for all data sets. All subsequent calculations of $\langle |B_R| \rangle$ are based on these 1-h averaged time series. We do, however, note that for the OMNI data set the field magnitude computed using the field vectors is approximately 10% lower than the measured scalar magnetic field, suggesting that high-frequency fluctuations do have an effect on the

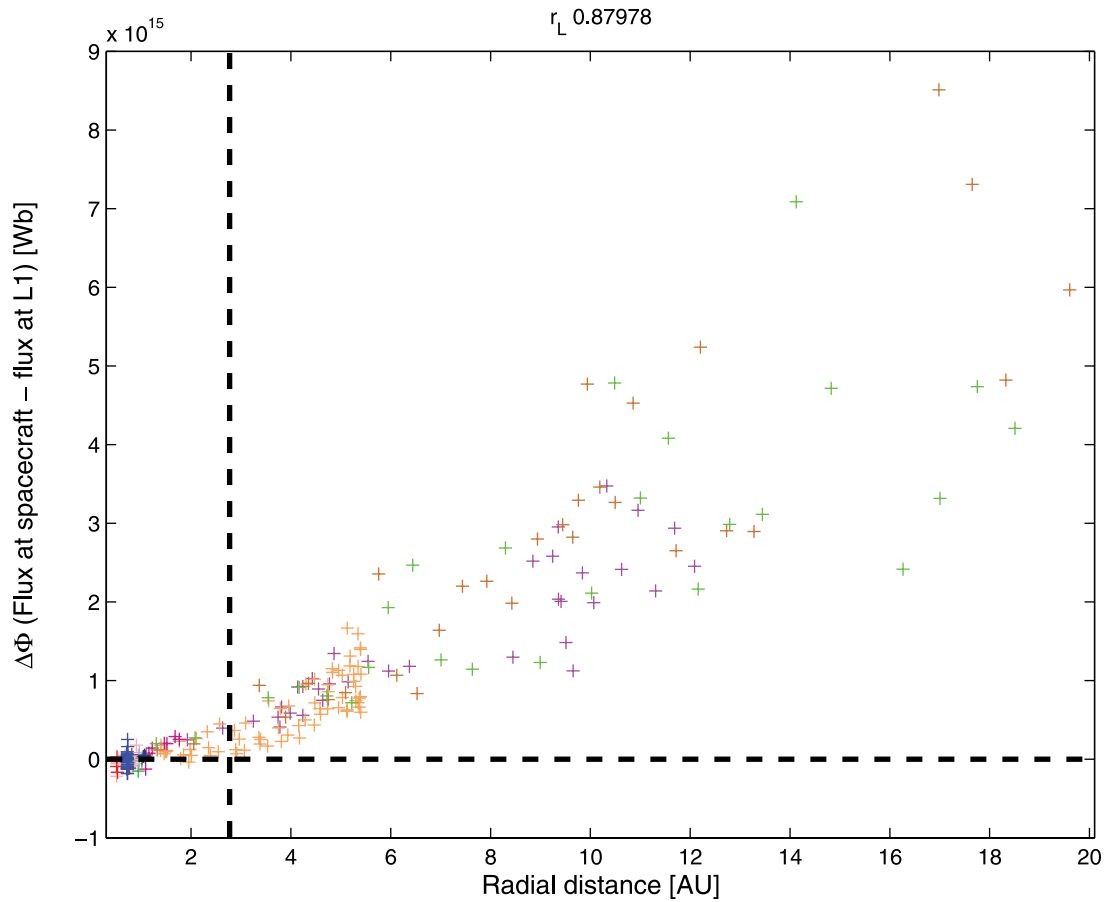


Figure 1. A plot of 3-Carrington-rotation averages of $\Delta\Phi$ (the difference between the near-Earth and far-Earth total heliospheric flux estimates) as a function of R (the heliocentric distance of the fE spacecraft). The color code for the various spacecraft is listed in Figure 2. Past $R = 2.5$ AU, the black dashed vertical line, there is a clear radial trend in $\Delta\Phi$.

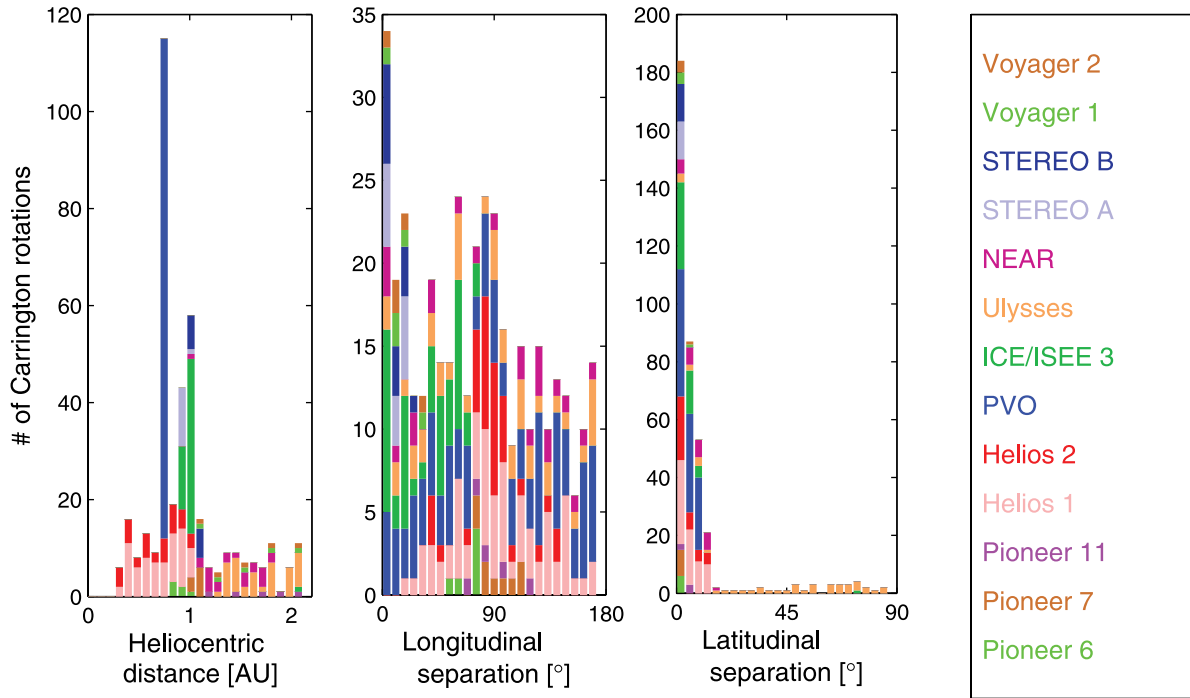


Figure 2. Histograms of the heliospheric coverage of the data used in this study, limiting $R < 2.5$ AU.

measured radial field. Thus, the flux calculated on the basis of $R^2 \langle |B_R| \rangle$ may be somewhat below the “true” value. By ensuring that all time averages are performed in the exact same manner, this effect will be the same for all the data sets considered and thus does not affect our assessment of single-point extrapolation to total heliospheric flux. We assume that all systematic instrumental offsets are well below the magnetic field variations under study.

2.2. Data Selection

[8] In order to compare estimates of total heliospheric flux from well-separated spacecraft in the heliosphere, we first use the OMNI data set (available from the National Space Science Data Center (NSSDC) at <http://omniweb.gsfc.nasa.gov/>) of spacecraft in near-Earth (nE) space to estimate the total heliospheric flux from 1963 through 2008. This nE flux estimate is compared to independent estimates from spacecraft well separated from Earth in heliocentric distance, latitude, or longitude, referred to as the far-Earth (fE) data points. Beginning with the NSSDC data sets, we select all available heliospheric magnetic field measurements from spacecraft at least 10° separated from Earth in heliolongitude and heliolatitude but within 20 AU. In addition to the NSSDC data, we also use near-Earth asteroid rendezvous (NEAR) magnetometer data, obtained from the Small Bodies Node of the Planetary Data System. The left-hand side of Table 1 lists the spacecraft fulfilling these criteria.

[9] To compare heliospheric flux estimates, we calculate the parameter $\Delta\Phi$, the difference between the cotemporal near-Earth and far-Earth total heliospheric flux estimates:

$$\Delta\Phi = 4\pi\text{AU}^2 (\langle |B_R| \rangle_{\text{nE}} - R^2 \langle |B_R| \rangle_{\text{fE}}), \quad (2)$$

where R is the heliocentric distance of the fE spacecraft. Figure 1 shows $\Delta\Phi$ as a function of R . The color code used to identify the different spacecraft is given in Figure 2. No correction for the solar wind transit time has been performed, but data points are 3-Carrington-rotation (i.e., ~ 80 -day) averages, so the effect should be insignificant except at the largest R values. Also, since it is the difference between the nE and fE flux estimate that is plotted, any global temporal variation should be subtracted out. Thus, the increase in $\Delta\Phi$ with R is a true, pronounced, radial variation (linear correlation coefficient of 0.87 beyond $R = 2.5$ AU). This trend is likely due to a reduced signal-to-noise ratio at large heliocentric distance (Smith, personal communication, 2008): the measured magnetic field will contain a noise contribution from fluctuations in the field, which for the radial component of the field arises from fluctuations in the azimuthal and meridional components. For simplicity, consider a Parker spiral magnetic field, in which there is no meridional component: B_R falls off as $1/R^2$, but the noise in B_R falls off as the azimuthal component of \mathbf{B} , which for a Parker spiral field is $(1/R) \cos \theta$, where θ is the heliolatitude. Thus, the noise contribution to the estimated total heliospheric flux, $4\pi R^2 |B_R|$, will vary as $R \cos \theta$. For the remainder of this study we only use data within 2.5 AU. The choice of this cut-off distance is somewhat arbitrary, but we note that below $R = 2.5$ AU the R dependence in $\Delta\Phi$ is less apparent.

2.3. Data Used

[10] To avoid the strong radial variation in the estimated heliospheric flux shown in Figure 1, the remainder of this study uses a subset of those data (listed in the right-hand side of Table 1) with the further constraint of $R < 2.5$ AU. Figure 2 shows histograms of the heliocentric distance and

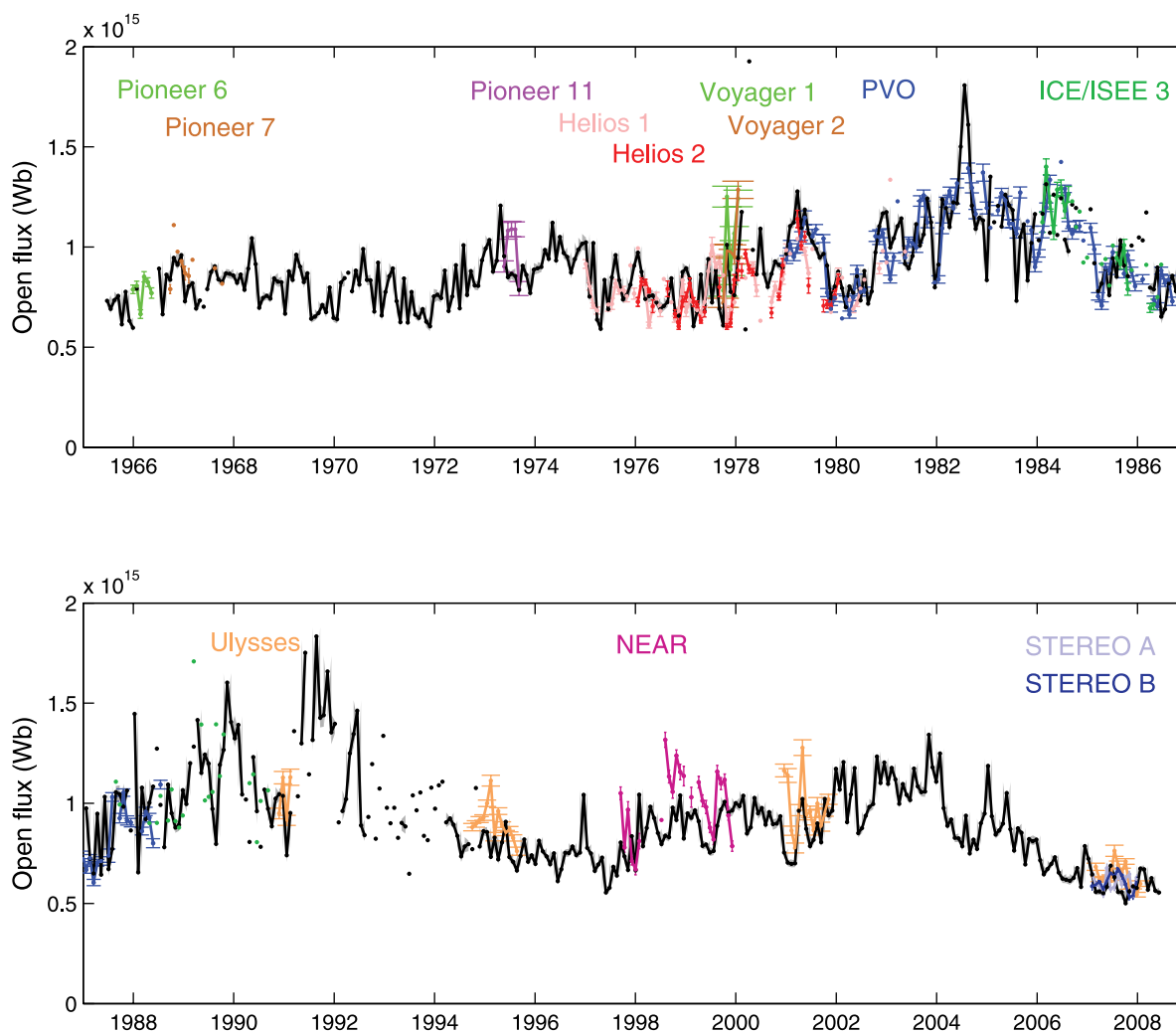


Figure 3. Time series of Carrington rotation averages of total heliospheric flux estimates based on magnetic field measurements at near-Earth (black) and far-Earth positions (colors are in the same format as in Figure 2). Connected lines (dots) show Carrington rotations with greater than one-third (one-fifth) data coverage.

angular separation from Earth (in heliographic longitude and latitude) at which the magnetic field measurements were made. Different spacecraft are identified by the colors shown to the right of the plots. While there is good coverage in heliocentric distance and heliographic longitude, coverage in heliographic latitude is generally limited to within $\sim 14^\circ$, with only Ulysses providing observations at more than 20° latitudinal separation from Earth.

3. Results

[11] In order to compare the total heliospheric flux observed by the spacecraft listed in Table 1 over a range of heliocentric latitudes and longitudes and within 2.5 AU, we plot Carrington rotation averages of total heliospheric flux estimates in Figure 3. Carrington rotation averages are used, as Lockwood *et al.* [2004] found no significant improvement in the correlation between ACE and Ulysses observations of $R^2|B_R|$ for longer averaging intervals. The color code is the same as in Figure 2. Error bars are standard

errors on the mean. Connected lines (dots) show Carrington rotations with greater than one-third (one-fifth) data coverage. For the 1965–2008 period, near-Earth (far-Earth) spacecraft provide at least one-fifth data coverage for 93% (44%) of the Carrington rotations considered.

[12] It can immediately be seen that there is good qualitative agreement between flux estimates made by well-separated spacecraft. The solar cycle variation in heliospheric flux inferred from single-point observations at L1 [e.g., Richardson *et al.*, 2002] is prevalent at all longitudes, latitudes, and heliocentric distances sampled, suggesting that it is indeed indicative in a change in the total heliospheric flux content. Even at solar maximum, the temporal changes in the Sun’s magnetic field do not result in different flux estimates from longitudinally separated spacecraft. The latitude invariance in $R^2|B_R|$ found during limited periods by comparing Ulysses and near-Earth observations [Smith and Balogh, 2003; Lockwood *et al.*, 2004] appears to hold for the extended time period, but smaller heliographic

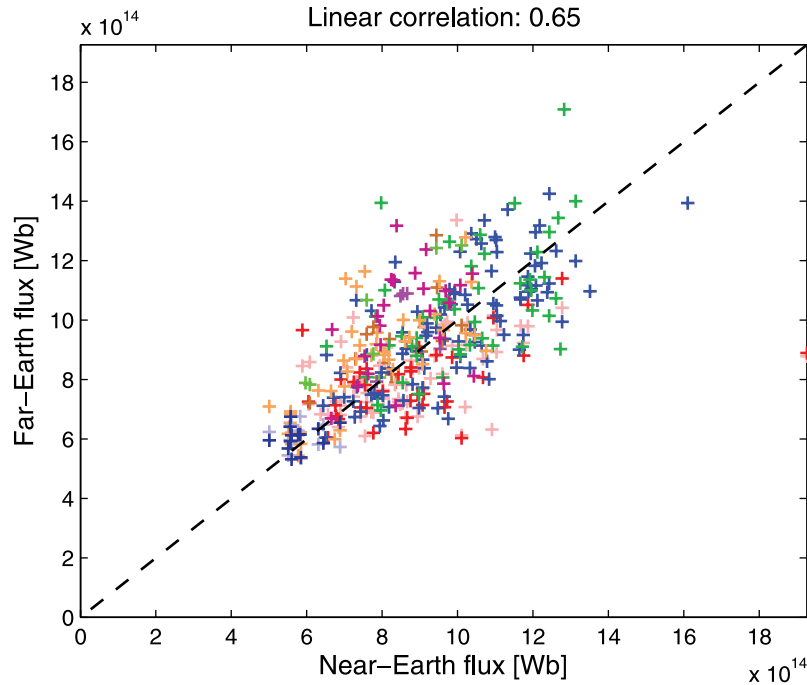


Figure 4. A scatterplot of Carrington rotation averages of total heliospheric flux estimates near Earth as a function of the cotemporal estimate at other far-Earth positions (colors are in the same format as in Figure 2). While there is significant spread about $y = x$, the black dashed line, there is still a strong correlation between the nE and fE estimates of heliospheric flux.

latitude excursions, additionally considered in this study. Furthermore, Figure 3 confirms that the time invariance in the Ulysses perihelion passes [Smith and Balogh, 2003] is the result of sampling the solar maximum flux during the Gnevyshev gap [Gnevyshev, 1977] and that the most recent (2008) perihelion pass shows a reduced flux, in agreement with the nE observations.

[13] Figure 4 shows a scatterplot of nE- and fE-derived total heliospheric flux estimates. The dashed line shows $y = x$, i.e., the same flux estimated near Earth and at large separations from Earth. As in Figure 3, there is good agreement between the nE and fE estimates of heliospheric flux. While there is considerable scatter about the $y = x$ line, the linear correlation coefficient (a linear relationship is expected between these parameters) is 0.65. For 371 data points involved in the correlation calculation, the null hypothesis that there is no correlation between the total flux estimates made by far-Earth and near-Earth spacecraft can be rejected above the 99% confidence level.

[14] Figure 5 shows scatterplots of $\Delta\Phi$, the difference between flux estimates made at nE and fE spacecraft, as a function of radial, longitudinal, and latitudinal separation from Earth. Top plots show the raw Carrington rotation averages, with spacecraft color codes as per Figure 2. Bottom plots show the data binned by R , latitude, and longitude. To highlight the smaller latitudinal separations, a logarithmic scale is used for the x axis of the latitude plot. There appears to be a weak trend (correlation coefficient 0.41) between $\Delta\Phi$ and R , passing through $\Delta\Phi = 0$ at $R = 1$ AU. This trend is the same as that shown in Figure 1. It suggests that total heliospheric flux estimates based on B_R

measurements 1 AU apart can differ by $\sim 10\%$. Latitude and longitude scatterplots, however, are centered on $\Delta\Phi = 0$ with no obvious trends (the slight increase in $\Delta\Phi$ for latitudes greater than 20° is due to only Ulysses data being considered and therefore skewed toward larger R). This suggests longitude and latitude invariance in flux, at least over these long (Carrington rotation) averages.

4. Conclusion

[15] We have estimated the total heliospheric flux at a number of well-separated points in the heliosphere, over four solar cycles. While large separations in heliographic latitude are only possible with perihelion passes of the Ulysses spacecraft, we are able to sample smaller latitudinal separations on a more routine basis by using the inclination of the ecliptic plane to the heliographic equator. For Carrington rotation averages, we find good agreement for all radial, longitudinal, and latitudinal separations throughout the solar cycle. The latitude invariance in $R^2|B_R|$, demonstrated during limited periods by the Ulysses observations [Smith and Balogh, 2003; Lockwood et al., 2004], appears to hold for the expanded time period considered in this study. As might be expected for such long time averages, we found longitudinal invariance in the estimated flux. For radial separations, however, there does still seem to be a weak trend for larger total heliospheric flux to be estimated on the basis of B_R observations at larger distances from the Sun. We suggest that this trend is due to the increasingly azimuthal field. Thus, we conclude that extrapolation of single-point measurements of the radial compo-

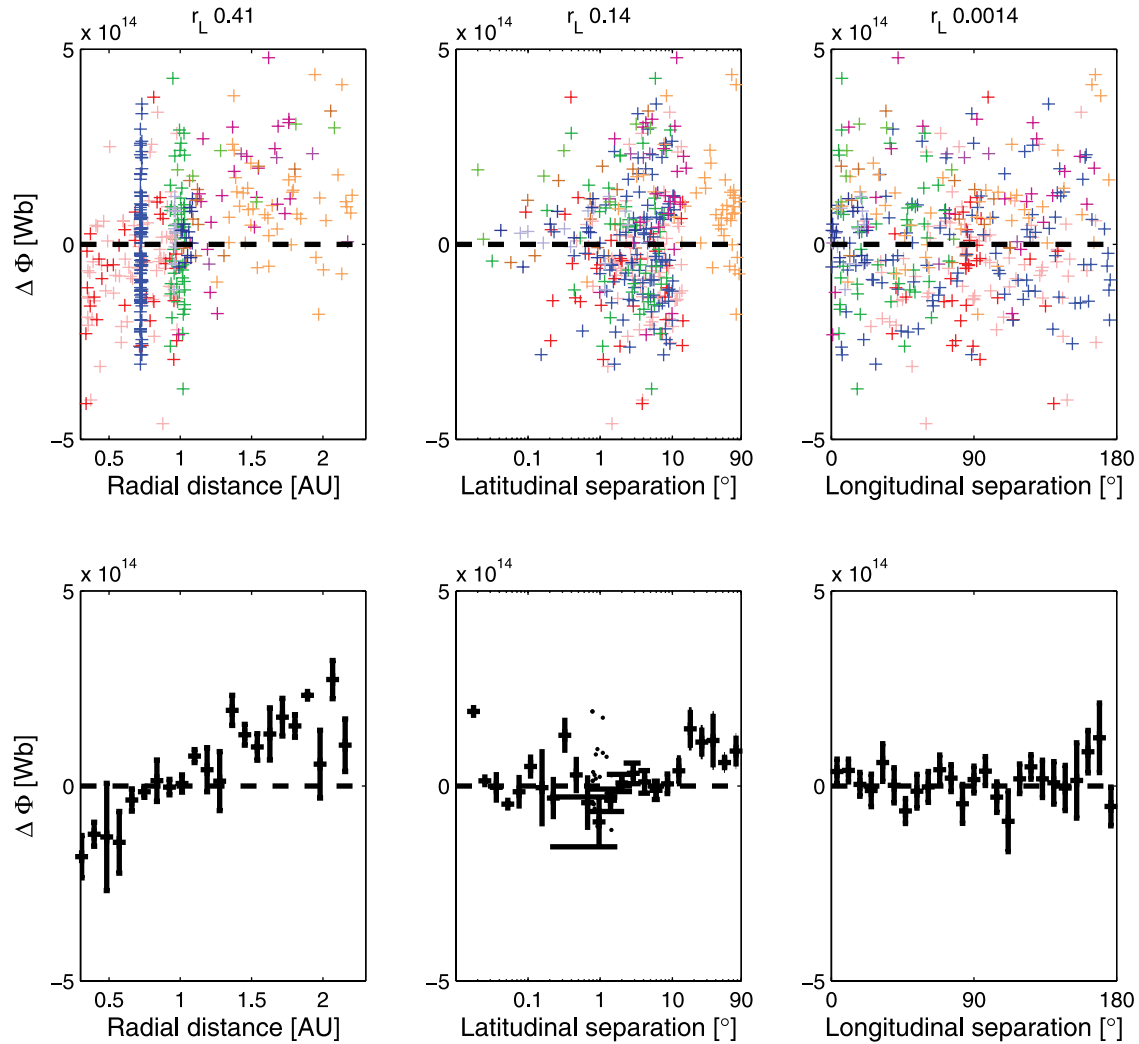


Figure 5. Scatterplots of $\Delta\Phi$, the difference between the total heliospheric flux estimates based on nE and fE observations, as a function of radial, longitudinal, and latitudinal separation. Top plots show the raw Carrington rotation averages, with spacecraft color code as per Figure 2. Bottom plots show the data binned by R , latitude, and longitude. To highlight the smaller latitudinal separations, a logarithmic scale is used for the x axis of the latitude plot. There are no obvious trends in the latitude or longitude scatterplots, but there does appear to be a weak correlation between estimated flux and heliocentric distance.

ment of the heliospheric magnetic field is a valid mean of estimating the total heliospheric magnetic flux in the inner heliosphere (inside ~ 2.5 AU), though care should be taken when comparing flux estimates at different heliocentric distances.

[16] **Acknowledgments.** This research was supported by the National Science Foundation under agreement ATM-012950, which funds the CISM project of the STC program. Research at Imperial College London was funded by STFC (UK), and NC was funded by NASA grant NNG06GC18G. We thank Tom Holzer for useful discussions. We are grateful to the Space Physics Data Facility and National Space Science Data Center for OMNI data and magnetic field data from Pioneer 6 and 7 (principal investigator N. Ness), Pioneer 10 and 11 (principal investigator E. Smith), Pioneer Venus Orbiter (principal investigator C. Russell), Helios (principal investigator N. Ness), Voyager (principal investigator L. Burlaga), ICE-ISEE3 (principal investigator E. Smith), Ulysses (principal investigator A. Balogh), and STEREO (principal investigator M. Acuña) and to the Small Bodies Node of the Planetary Data System for NEAR magnetometer data (principal investigator M. Acuña).

[17] Amitava Bhattacharjee thanks Susan T. Lepri and Leif Svalgaard for their assistance in evaluating this paper.

References

- Acuña, M. H., C. T. Russell, L. J. Zanetti, and B. J. Anderson (1997), The NEAR magnetic field investigation: Science objectives at asteroid Eros 433 and experimental approach, *J. Geophys. Res.*, *102*, 23,751–23,759, doi:10.1029/97JE01161.
- Acuña, M. H., D. Curtis, J. L. Scheifele, C. T. Russell, P. Schroeder, A. Szabo, and J. G. Luhmann (2007), The STEREO/IMPACT magnetic field experiment, *Space Sci. Rev.*, *136*, 203–226, doi:10.1007/s11214-007-9259-2.
- Altschuler, M. A., and G. Newkirk Jr. (1969), Magnetic fields and the structure of the solar corona, *Sol. Phys.*, *9*, 131–149.
- Babcock, H. W. (1961), The topology of the Sun's magnetic field and the 22-year cycle, *Astrophys. J.*, *133*, 527–587.
- Balogh, A., T. J. Beek, R. J. Forsyth, P. C. Hedgecock, R. J. Marquedant, E. J. Smith, D. J. Southwood, and B. T. Tsurutani (1992), The magnetic field investigation on the Ulysses mission: Instrumentation and preliminary scientific results, *Astron. Astrophys. Suppl. Ser.*, *92*, 221–236.
- Behannon, K. W., M. H. Acuna, L. F. Burlaga, R. P. Lepping, N. F. Ness, and F. M. Neubauer (1977), Magnetic field experiment for Voyagers 1 and 2, *Space Sci. Rev.*, *21*, 235–257.

- Crooker, N. U., J. T. Gosling, and S. W. Kahler (2002), Reducing heliospheric magnetic flux from coronal mass ejections without disconnection, *J. Geophys. Res.*, *107*(A2), 1028, doi:10.1029/2001JA000236.
- Fisk, L. A., and N. A. Schwadron (2001), The behaviour of the open magnetic field of the Sun, *Astrophys. J.*, *560*, 425–438.
- Fisk, L. A., T. H. Zurbuchen, and N. A. Schwadron (1999), Coronal hole boundaries and their interaction with adjacent regions, *Space Sci. Rev.*, *87*, 43–54.
- Frandsen, A. M. A., B. V. Connor, J. van Amersfoort, and E. J. Smith (1978), The ISEE-C vector helium magnetometer, *IEEE Trans. Geosci. Electron.*, *16*, 195–198.
- Gnevyshev, M. N. (1977), Essential features of the 11-year solar cycle, *Sol. Phys.*, *51*, 175–183.
- Jones, G. H., A. Balogh, and E. J. Smith (2003), Solar magnetic field reversal as seen at Ulysses, *Geophys. Res. Lett.*, *30*(19), 8028, doi:10.1029/2003GL017204.
- Lepri, S. T., S. K. Antiochos, P. Riley, L. Zhao, and T. H. Zurbuchen (2008), Comparison of heliospheric in situ data with the quasi-steady solar wind models, *Astrophys. J.*, *674*, 1158–1166, doi:10.1086/524347.
- Levine, R. H., M. D. Altschuler, and J. W. Harvey (1977), Solar sources of the interplanetary magnetic field and solar wind, *J. Geophys. Res.*, *82*, 1061–1065.
- Linker, J. A., Z. Mikić, D. A. Biesecker, R. J. Forsyth, S. E. Gibson, A. J. Lazarus, A. Lecinski, P. Riley, A. Szabo, and B. J. Thompson (1999), Magnetohydrodynamic modeling of the solar corona during Whole Sun Month, *J. Geophys. Res.*, *104*, 9809–9830.
- Lockwood, M., R. Stamper, and M. N. Wild (1999), A doubling of the Sun's coronal magnetic field during the past 100 years, *Nature*, *399*, 437–439, doi:10.1038/20867.
- Lockwood, M., R. J. Forsyth, A. Balogh, and D. J. McComas (2004), Open solar flux estimates from near-Earth measurements of the interplanetary magnetic field: Comparison of the first two perihelion passes of the Ulysses spacecraft, *Ann. Geophys.*, *22*, 1395–1405.
- Low, B. C. (2001), Coronal mass ejections, magnetic flux ropes, and solar magnetism, *J. Geophys. Res.*, *106*, 25,141–25,160.
- Mikić, Z., J. A. Linker, D. D. Schnack, R. Lionello, and A. Tarditi (1999), Magnetohydrodynamic modeling of the global solar corona, *Phys. Plasmas*, *6*, 2217–2224.
- Ness, N. F., C. S. Scearce, and S. C. Cantarano (1966), Preliminary results from the Pioneer 6 magnetic field experiment, *J. Geophys. Res.*, *71*, 3305–3313.
- Owens, M. J., and N. U. Crooker (2006), Coronal mass ejections and magnetic flux buildup in the heliosphere, *J. Geophys. Res.*, *111*, A10104, doi:10.1029/2006JA011641.
- Owens, M. J., and N. U. Crooker (2007), Reconciling the electron counterstreaming and dropout occurrence rates with the heliospheric flux budget, *J. Geophys. Res.*, *112*, A06106, doi:10.1029/2006JA012159.
- Owens, M. J., N. A. Schwadron, N. U. Crooker, W. J. Hughes, and H. E. Spence (2007), Role of coronal mass ejections in the heliospheric Hale cycle, *Geophys. Res. Lett.*, *34*, L06104, doi:10.1029/2006GL028795.
- Owens, M. J., H. E. Spence, S. McGregor, W. J. Hughes, J. M. Quinn, C. N. Arge, P. Riley, J. Linker, and D. Odstrcil (2008), Metrics for solar wind prediction models: Comparison of empirical, hybrid, and physics-based schemes with 8 years of L1 observations, *Space Weather*, *6*, S08001, doi:10.1029/2007SW000380.
- Richardson, I. G., H. V. Cane, and E. W. Cliver (2002), Sources of geomagnetic activity during nearly three solar cycles (1972–2000), *J. Geophys. Res.*, *107*(A8), 1187, doi:10.1029/2001JA000504.
- Russell, C. T., R. C. Snare, J. D. Means, and R. C. Elphic (1980), Pioneer Venus Orbiter fluxgate magnetometer, *IEEE Trans. Geosci. Remote Sens.*, *GE-18*, 32–35.
- Scearce, C., S. Cantarano, N. Ness, F. Mariani, R. Terenzi, and L. Burlaga (1975), The Rome-GSFC magnetic field experiment for Helios A and B (E3), *Tech. Rep. X-692-75-112*, NASA Goddard Space Flight Cent., Greenbelt, Md.
- Schatten, K. H., J. M. Wilcox, and N. F. Ness (1969), A model of interplanetary and coronal magnetic fields, *Sol. Phys.*, *9*, 442–455.
- Smith, E. J., and A. Balogh (2003), Open magnetic flux: Variation with latitude and solar cycle, in *Solar Wind Ten*, edited by M. Velli, R. Bruno, and F. Malara, AIP Conf. Proc., 679, 67–70.
- Smith, E. J., B. V. Connor, and G. T. Foster Jr. (1975), Measuring the magnetic fields of Jupiter and the outer solar system, *IEEE Trans. Magn.*, *11*, 962–980.
- Svalgaard, L., and E. W. Cliver (2007), A floor in the solar wind magnetic field, *Astrophys. J.*, *661*, L203–L206, doi:10.1086/518786.
- Svalgaard, L., T. L. Duvall Jr., and P. H. Scherrer (1978), The strength of the Sun's polar fields, *Sol. Phys.*, *58*, 225–239.
- Ulrich, R. K. (1992), Analysis of magnetic fluxtubes on the solar surface from observations at Mt. Wilson of A5250; A5233, in *Cool Stars, Stellar Systems, and the Sun*, *Astron. Soc. Pac. Conf. Ser.*, vol. 26, edited by M. S. Giampapa and J. A. Bookbinder, pp. 265–267, Astron. Soc. of the Pac., San Francisco, Calif.
- Wang, Y.-M., and N. R. Sheeley Jr. (1995), Solar implications of Ulysses interplanetary field measurements, *Astrophys. J.*, *447*, L143–L146, doi:10.1086/309578.
- Wang, Y.-M., and N. R. Sheeley Jr. (2003), On the topological evolution of the coronal magnetic field during the solar cycle, *Astrophys. J.*, *599*, 1404–1417.
- Wang, Y.-M., S. H. Hawley, and N. R. Sheeley Jr. (1996), The magnetic nature of coronal holes, *Science*, *271*, 464–469.

C. N. Arge, Space Vehicles Directorate, Air Force Research Laboratory, Kirtland Air Force Base, NM 87117, USA.

N. U. Crooker and N. A. Schwadron, Center for Space Physics, Boston University, Boston, MA 02215, USA.

T. S. Horbury and M. J. Owens, Space and Atmospheric Physics, Blackett Laboratory, Imperial College London, London, SW7 2BW, UK. (m.owens@imperial.ac.uk)